

IMPACT-ANGLE CONTROL OF ASTEROID INTERCEPTORS/PENETRATORS

Matt Hawkins* and Bong Wie†

Many of the possible asteroid threat mitigation techniques call for the use of nuclear explosives to effect disruption of near-Earth objects. Such techniques impart as much momentum to the dispersed particles as possible. Subsurface nuclear explosions are the most effective option, but need to place the nuclear device as far under the surface as possible to maximize the amount of energy coupled from the nuclear device to the body. A guidance technique involving statistical orbit determination is discussed, and added as an option to an existing simulator for terminal-phase guidance. The asteroid Apophis is used as an illustrative example to show that a variety of nuclear penetrator missions are possible. A guidance scheme to change a spacecraft's approach angle towards the end of the mission for a low relative velocity is analyzed. A model for a new scenario, a leading kinetic-impact spacecraft followed several seconds later by a spacecraft with the nuclear payload, is described. Simulation results show that this new scenario may be promising, and factors that warrant further research are identified. The guidance schemes analyzed in this paper contribute to a simulator program with many options for different asteroid missions.

INTRODUCTION

The potential threat to planet Earth from the impact of an asteroid has been recognized for a few decades. The scientific community has been engaged in identifying and characterizing hazardous near-Earth objects, and studying various techniques to mitigate the threat.¹ Studies of deflection techniques show that fragmentation is possible for all but the lowest-energy methods.^{2,3} Current research is focused on predicting the likely trajectories of the dispersed cloud of fragments for a variety of high-energy nuclear explosive deflection scenarios.⁴

Once suitable parameters for a nuclear deflection mission are identified, the challenge is to deliver a nuclear payload to the asteroid. NASA's Deep Impact mission provided an impressive demonstration of the current state of the art in spacecraft guidance, successfully delivering an autonomous impactor to comet Tempel 1, while an autonomous flyby vehicle observed the impact event.⁵ This mission success shows that sophisticated hardware and software are available for challenging mission designs. A simulation of a guidance law for a Deep Impact-type spacecraft demonstrates the technique.

*Graduate Research Assistant, Asteroid Deflection Research Center, Department of Aerospace Engineering, Iowa State University, 2271 Howe Hall, Ames, IA 50011-2271.

†Vance Coffman Endowed Chair Professor, Asteroid Deflection Research Center, Department of Aerospace Engineering, Iowa State University, 2271 Howe Hall, Ames, IA 50011-2271.

Dispersal simulations⁴ show that the effectiveness of a nuclear disruption in minimizing the mass fraction of the asteroid that eventually impacts Earth depends heavily on the intercept angle of the nuclear device. Furthermore, subsurface nuclear explosions are far more effective than surface or standoff explosions, with the implication that a good intercept mission design will be able to deliver a subsurface nuclear device at some specified intercept angle. The term intercept angle is used here without precise definition. The various angles which characterize the mission are defined later.

Three different broad classes of intercept mission are analyzed. The first is a simple intercept with Deep Impact-type guidance capabilities. The second type is impact with a controlled intercept angle. For low relative impact velocities it is feasible to carry enough fuel onboard to significantly change the intercept angle even in the terminal phase of the mission, as a reaction to current conditions or to change from the nominal mission design. The third is a high-speed impact with two spacecraft in a leader-follower configuration. The leader will bore a hole through the asteroid, allowing a follower to deliver a nuclear payload several meters under the surface. The three mission types are simulated and the performance of the guidance laws is analyzed.

DYNAMICAL MODEL AND MISSION SCENARIO

Dynamical Model

A target asteroid is modeled as a point mass in a heliocentric Keplerian orbit described by

$$\ddot{\vec{R}}_T + \frac{\mu_{\odot}}{R_T^3} \vec{R}_T = 0 \quad (1)$$

where \vec{R}_T is the position vector of the target asteroid from the sun, and $\mu_{\odot} = 1.32715 \times 10^{20} \text{ m}^3/\text{s}^2$ is the solar gravitational parameter. The heliocentric orbital motion of the interceptor spacecraft is described by

$$\ddot{\vec{R}}_S + \frac{\mu_{\odot}}{R_S^3} \vec{R}_S - \frac{\mu_{\otimes}}{R^3} \vec{R} = \vec{f} \quad (2)$$

where \vec{R}_S is the position vector of the spacecraft from the sun, $\mu_{\otimes} \simeq 15.35 \text{ m}^3/\text{s}^2$ is an estimated gravitational parameter for Apophis, and \vec{f} is the sum of the perturbing force vectors (per unit mass) acting on the spacecraft. In this paper only forces from the commanded accelerations are considered for trajectory propagation dynamics.

The relative target-spacecraft separation is described by

$$\vec{R} = \vec{R}_T - \vec{R}_S \quad (3)$$

where \vec{R} is the position vector of the target from the spacecraft.

From Figure 1 it can be seen that

$$\lambda = \arctan \frac{R_y}{R_x} \quad (4)$$

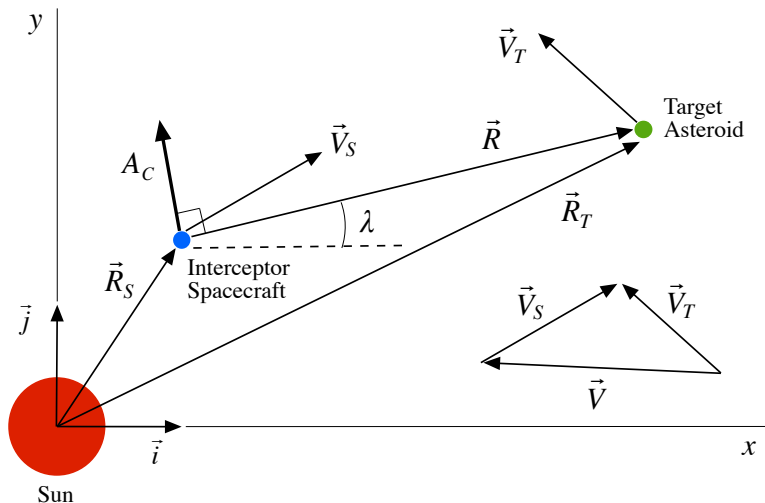


Figure 1. Two-dimensional intercept geometry.

where λ is the line-of-sight (LOS) angle, and (R_x, R_y) are the components of the relative position vector along the inertial (x, y) coordinates. Differentiating this with respect to time gives

$$\dot{\lambda} = \frac{R_x V_y - R_y V_x}{R^2} \quad (5)$$

where $\dot{\lambda}$ is the LOS rate, $R = (R_x^2 + R_y^2)^{\frac{1}{2}}$, and the relative velocity components are found, by differentiating the relative position components, as follows:

$$V_x = \dot{R}_x \quad (6)$$

$$V_y = \dot{R}_y \quad (7)$$

Similarly, the velocity components for the spacecraft and target are found as follows:

$$V_{S_x} = \dot{R}_{S_x} \quad (8)$$

$$V_{S_y} = \dot{R}_{S_y} \quad (9)$$

$$V_{T_x} = \dot{R}_{T_x} \quad (10)$$

$$V_{T_y} = \dot{R}_{T_y} \quad (11)$$

To describe and analyze various aspects of the intercept problem, it is useful to define several angles. The first of these is the phase angle, which astronomers traditionally define as the Sun-object-Earth angle, that is, the angle between the Sun and the Earth as seen from the object. For space missions this is generalized to the Sun-object-spacecraft angle. The phase angle is 0° when the spacecraft is between the Sun and the target object, resulting in a fully illuminated object. It is 90° when the object is half-illuminated (a sphere will

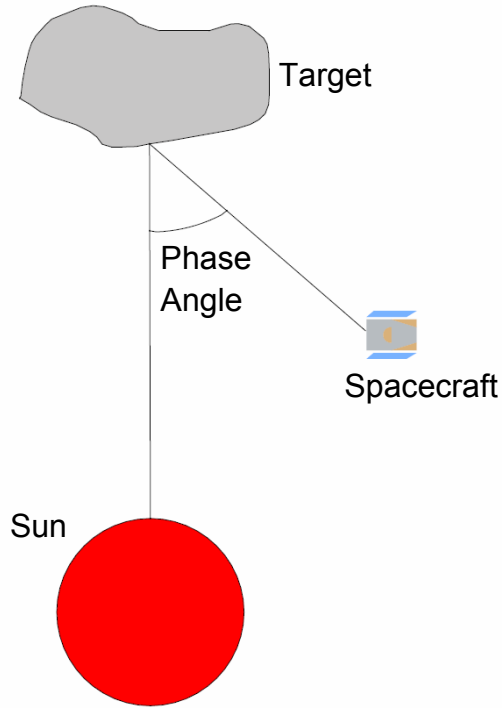


Figure 2. Phase angle.

appear like a first or last quarter moon), and 180° when the object is between the Sun and the spacecraft, resulting in minimal illumination. Figure 2 shows the phase angle.

Another useful angle is the approach angle. In this paper the approach angle is defined as the angle between the target’s heliocentric velocity vector and the velocity vector of the spacecraft relative to the target. With this definition, a 0° approach angle corresponds to an “arrive-from-behind” impact, with the target and spacecraft velocities aligned at impact. An approach angle of 180° corresponds to an “arrive from ahead” impact. Positive approach angles correspond to impacts from outside the target orbit, and negative angles come from inside the orbit. Figure 3 shows the approach angle.

Finally, the impact angle is used to characterize the direction of the impact from the target’s local vertical. This angle assumes a spherical target of known radius, while real asteroids are in general irregularly shaped. However, the impact angle is still a useful way to quantify performance for this preliminary study of impact-angle control. An impact angle of 0° corresponds to a direct hit, with a velocity vector which would intercept the center of mass. Higher impact angles correspond to “glancing blows,” with a 90° impact angle hitting tangential to the surface. Figure 4 shows the impact angle.

Asteroid 99942 Apophis

The asteroid 99942 Apophis is used as an example target asteroid in this paper. Apophis has garnered much attention due to the possibility of a so-called keyhole passage on April

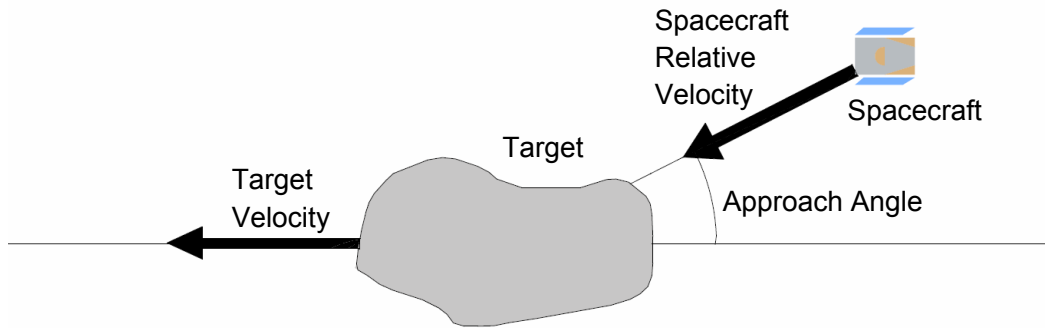


Figure 3. Approach Angle.

13, 2029. [6] The probability of keyhole passage is now estimated to be much lower than initial estimates, but Apophis is still of interest due to its future approaches near the Earth.

The terminal phase of a mission starts when measurements of the target can be taken, sometime after the target is in visible sensor range. During the terminal phase, velocity corrections are computed to correct for errors in the initial orbit injection. For the Apophis scenario in this paper, the terminal phase begins 24 hours before nominal intercept time. For this analysis, Apophis will be treated as a sphere with a diameter of 270 m, as given in JPL’s small-body database.

Apophis is an Aten-class asteroid with an orbital semi-major axis less than 1 AU. Its orbital period about the sun is 323 days. Table 1 gives the six classical orbital elements of Apophis in JPL 140 (heliocentric ecliptic J2000 reference frame at epoch JD 2455400.5 (2010-July-23.0) TDB). Other orbital characteristics are estimated as: perihelion $r_p = 0.74606$ AU, aphelion $r_a = 1.09881$ AU, perihelion speed $V_p = 37.6$ km/s, aphelion speed $V_a = 25.5$ km/s, perihelion passage time $t_p = \text{JD } 2455542.06$ (2010-Dec-11.56), mean orbital rate $n = 2.2515 \times 10^{-7}$ rad/s, and mean orbital speed = 30.73 km/s.

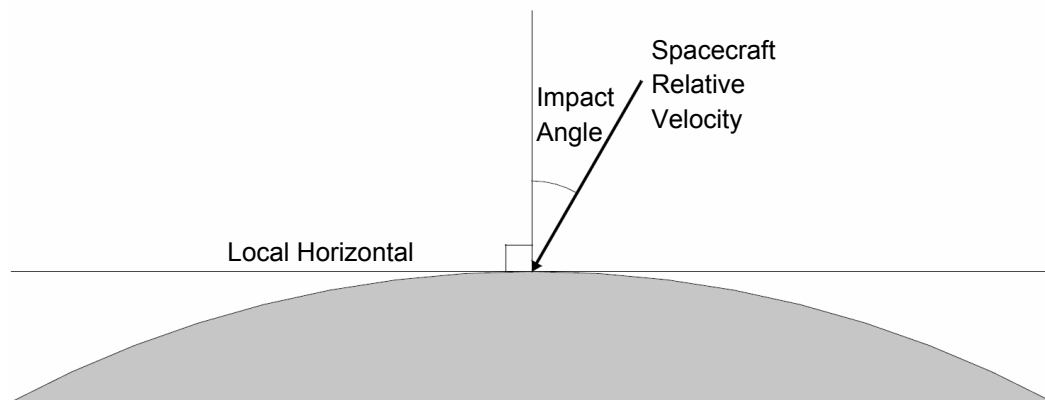


Figure 4. Impact Angle.

Table 1. Orbital elements of asteroid Apophis at Epoch 2455400.5 (2010-July-23.0) TDB. Source: JPL’s small-body database.

Orbital Elements	Value
Semimajor axis a , AU	0.9223
Eccentricity e	0.1911
Inclination i , deg	3.3317
Perihelion argument ω , deg	126.4186
Right ascension longitude Ω , deg	204.4320
Mean anomaly M_0 , deg	202.4953

Intercept Mission Scenarios

Requirements and restrictions on asteroid missions may vary widely, depending on factors such as mission lead time, ΔV capability, impact velocity, and payload mass. Because of the wide variety within the group of potentially hazardous objects and the range of different impact options, there is no one-size-fits-all mission scenario. Three different primary intercept mission scenarios are examined in this paper.

In all three scenarios, the terminal phase begins with Apophis at perihelion, with nominal impact time 24 hours later. Specifying the approach angle and relative impact velocity suffices to determine the initial conditions for a spacecraft on course to intercept after 24 hours. Missions will usually be specified by these two quantities, with reference to other angles or characteristics as needed.

The first mission type is a simple intercept mission to add Deep Impact-type guidance capabilities to a previously developed mission simulation program.⁷ The performance of this type of guidance logic is analyzed, and the guidance scheme is added to the simulation program.

The second mission type looks to control the approach angle for low-speed (50 to 300 m/s) relative impact velocities. The spacecraft is commanded to change the approach angle by up to 90° from the nominal approach angle during the terminal phase.

The third mission type is a high-speed impact for two spacecraft in a leader-follower configuration. To effectively deliver a nuclear payload well beneath the surface of the target asteroid, a spacecraft will need to bore through the asteroid before detonation of the nuclear device. Using a separate penetrator spacecraft followed closely by the spacecraft with the nuclear payload has some potential advantages over carrying everything on the same self-contained craft.

MISSIONS

Orbit Determination Guidance

NASA’s Deep Impact mission sent impactor and flyby spacecraft to comet Tempel 1 with the goal of impacting the comet’s nucleus at a high (10 km/s) impact velocity, with a flyby spacecraft observing the event. Intercept was successfully achieved on July 4, 2005.⁵ The flyby spacecraft successfully observed the event, although some observations were obscured

by an unexpectedly large ejecta plume. The Deep Impact mission used AutoNav software, originally developed for Deep Space 1, for both navigation of the impactor and control of the flyby spacecraft’s observations.⁸

NASA’s AutoNav software⁹ uses statistical orbit determination to determine the position and velocity of both the spacecraft and the target from onboard observations. During the cruise phase of the mission, a Kalman filter uses observations of known bodies to determine the spacecraft’s orbit in heliocentric inertial coordinates. During the terminal phase, observations of the target are used to compute a relative trajectory. AutoNav includes routines for image processing, orbit determination, and maneuver computations.

A simplified model for orbit determination control was developed and simulated for the Apophis example. In practice the orbit determination process is used to estimate the orbits of the spacecraft and the target. For this example, the orbits of the spacecraft and target are assumed to be known as a result of orbit determination, and a guidance law is needed to compensate for errors in the terminal injection conditions.

Orbit determination guidance, as described in this paper, is a Lambert guidance scheme using the orbits of the spacecraft and the target. Lambert’s problem can be formulated as: given two position vectors (end points) and the travel time, find the velocities at these end points. For the intercept problem, the beginning point can be taken as the spacecraft’s current position, and the endpoint the target’s position at impact. Solution of Lambert’s problem will then yield the required velocity to put the spacecraft on an intercepting orbit.

When a maneuver is to be performed, the time-to-go is first calculated from the closing velocity and target range. The target’s current state (position and velocity) is integrated to find the target’s position at the estimated end of flight time. The spacecraft’s current position, the target’s nominal end-of-flight position, and the time-to-go are given as inputs to a Lambert solver routine. The Lambert solver gives as output the velocity vector for the orbit connecting the spacecraft’s position and the nominal end-of-flight target position over the time-to-go. The initial velocity from the Lambert solution is denoted as $\vec{V}_{Lambert}$.

The required velocity change is given as

$$\Delta\vec{V} = \vec{V}_{Lambert} - \vec{V}_S \tag{12}$$

The time-to-go is calculated from a linearized range equation using the current relative position and velocity, and is thus imprecise, and may change when a maneuver is performed. The target position will thus be calculated for an incorrect time of flight and will differ from its eventual location at impact. Low-thrust divert thrusters do not apply instantaneous acceleration, but rather take some finite amount of time to apply. As the spacecraft continues to move during thruster firing, the actual velocity change imparted will not exactly match the velocity change specified by the guidance routine.

These two error sources cause degraded performance near the end of the terminal mission phase. However, as time-to-go decreases, the perturbing effects of gravity on the spacecraft’s and target’s trajectories decrease. Therefore at the end of the terminal mission phase, with t_{go} the nominal mission time-to-go, linear dynamics are assumed and the required velocity change is simply

$$\Delta\vec{V} = \frac{\vec{R}}{t_{go}} - \vec{V} \quad (13)$$

Impact Angle Guidance

A number of guidance laws can be used to successfully intercept an asteroid, even at high relative impact velocities on the order of 10 km/s or more. These laws will result in an intercept at the approach angle specified by the mission design. Different mission requirements and designs may benefit from or even depend on impacting the asteroid at a different angle than the nominal angle from the mission design. Fuel requirements make impact angle guidance impractical for high-speed impacts, but for encounters with relative velocities in the low 100s of m/s a wide range of impact angles can be commanded.

Typical impact-angle control guidance laws have been developed for guided missiles.¹⁰ Guided missiles typically effect commanded accelerations by aerodynamic lift from control surfaces. Although there may be limits on maneuverability, the control energy is essentially free. For a spacecraft, however, all acceleration is provided by fuel, which must be carried onboard and takes up precious payload space and mass. Fuel requirements are the fundamental limiting factor to how significantly a spacecraft can change its orbit.

Reference 11 gives a formulation for a trajectory-shaping guidance law with a constant acceleration target maneuver. The target asteroid will experience acceleration due to the sun's gravity, and for the short timescale of terminal encounter this acceleration can be treated as constant. This guidance law also minimizes the required fuel. The goal, then, is to command impact at a given velocity, described by

$$\vec{R}(t_f) = 0 \quad (14)$$

$$\dot{\vec{R}}(t_f) = \dot{\vec{R}}_f \quad (15)$$

$$(16)$$

with minimum commanded acceleration, namely

$$\min_{A_c} \int_{t_0}^{t_f} A_c(t)^2 dt \quad (17)$$

where A_c is the commanded acceleration.

Solving this optimal control problem and working in terms of the line of sight angle gives the acceleration commands as¹¹

$$A_c = 4V_c\dot{\lambda} + \frac{2V_c(\lambda - \lambda_f)}{t_{go}} + A_T \quad (18)$$

where V_c is the closing velocity, λ_f is the commanded line-of-sight angle at impact, and A_T is the target's acceleration.

Leader/Follower Subsurface Nuclear Penetrator

A number of recent studies^{3,4,12} have shown that delivering a nuclear explosive to an asteroid will result in the most deflection for a given payload size. The most deflection corresponds to the greatest velocity change when the asteroid is simply pushed off its current trajectory. For nuclear devices, fragmentation is possible, so the most deflection in this case corresponds to having the smallest fraction of the original asteroid's mass intercept the earth. Reference 4 has shown that sufficient fragmentation velocities result in very small mass fractions intercepting the earth, even for last-minute deflection attempts.

The average velocity change for disrupted particles increases greatly between a standoff nuclear explosion and a surface explosion, and again between a surface explosion and a subsurface explosion. For a subsurface explosion, increasing the depth at which the device is buried results in increased energy coupling¹³ and thus increased velocity of the fragmented particles. In other words, the deeper the device is buried the better. The decision to utilize a subsurface nuclear explosion, then, raises the question of how best to deliver a nuclear payload below the surface of the asteroid.

Reference 12 describes proposed methods for delivering a subsurface nuclear payload. One method is to have a striker consisting of a spherical leader which is 4 meters in front of a conical nuclear charge device. The leader sweeps out asteroid material allowing the charge to explode deeper inside the asteroid. The evaporated material can cause huge pressure spikes on the nuclear device, though, likely preventing normal operation of the device. The second method places a complex shield immediately in front of the charge cone to sweep out the material. This results in reduced interference by the leader on the charge cone by enforcing more physical separation between the swept out material and the charge cone.

One option for increasing the depth of the nuclear device is to utilize a separate penetrator spacecraft as a leader to sweep out material slightly before the nuclear device arrives. The nuclear device will arrive in a follower spacecraft. Using separate spacecraft allows significantly more time for pressure disturbance effects to settle, allowing the nuclear device a clean opening through the asteroid. Figure 5 shows the overall mission operations for the leader/follower concept. As will be discussed in the results section, there are not any well-established values for parameters like separation time, separation velocity, and following distance, so this diagram should be considered purely schematic.

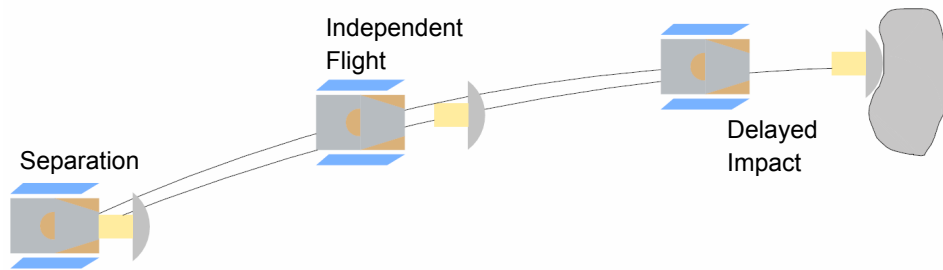


Figure 5. Schematic overview of leader-follower mission.

At the determined separation time, the two coupled spacecraft will separate via either pyrotechnic devices or a spring release mechanism. The separate craft will fly under the guidance of either separate guidance systems or by one craft calculating guidance commands

for both. In a successful mission the leading penetrator craft will hit the target asteroid, followed several seconds later by the following spacecraft placing a nuclear payload deep under the surface of the asteroid.

If the time delay required is such that the two spacecraft do not need to be more than about 100 meters apart, the penetrator and nuclear device could be carried on the same spacecraft, with the penetrator placed ahead of the nuclear payload by means of an extendable boom. A long boom would relieve the difficulties of coordinating two spacecraft, at the expense of a more complicated attitude control problem. Figure 6 shows the overall mission operations for the extendable boom concept.

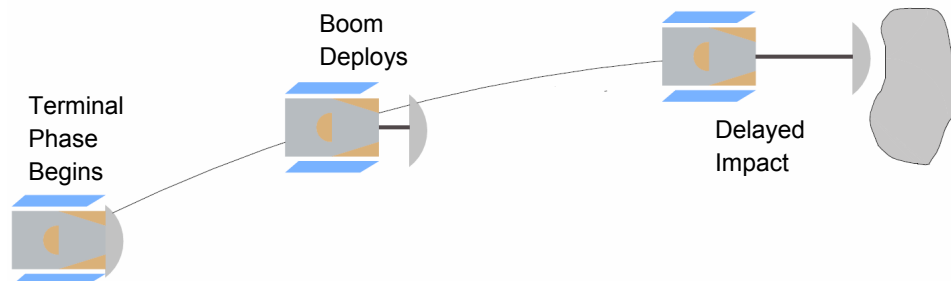


Figure 6. Schematic overview of boom deployment mission.

This paper is not concerned with the attitude dynamics of such a large structure. The guidance basic guidance laws for a single spacecraft should suffice to guide the spacecraft with deployed boom to the asteroid given a sufficiently sophisticated attitude control system.

SIMULATION RESULTS

The guidance laws for the three mission scenarios described were simulated with a 4th-order Runge Kutta numerical integration scheme. The baseline spacecraft is assumed to be a 1000-kg interceptor with 10 N thrusters. It is assumed that positions and velocities of the target and spacecraft are available with no errors.

Orbit Determination Guidance

The orbit determination guidance scheme was simulated for initial conditions used for previous guidance law simulation.⁷ These initial conditions result in a 10.8 km/s closing velocity, and a miss distance of 40,000 km in the absence of guidance commands. These initial conditions are provided in Table 2. The performance of this guidance law and others from the previous study, in terms of Δv and miss distance (also called Zero Effort Miss, ZEM) are given in Table 3. Trajectories of the spacecraft and target, line-of-sight and line-of-sight rate histories, and Δv usage are shown in Figures 7 and 8.

The values for Δv usage and miss distance compare favorably with other guidance schemes. Furthermore, the information available from an orbit determination system can give reliable estimates of heliocentric position and velocity, which can be utilized in different ways for a number of different deflection scenario options.

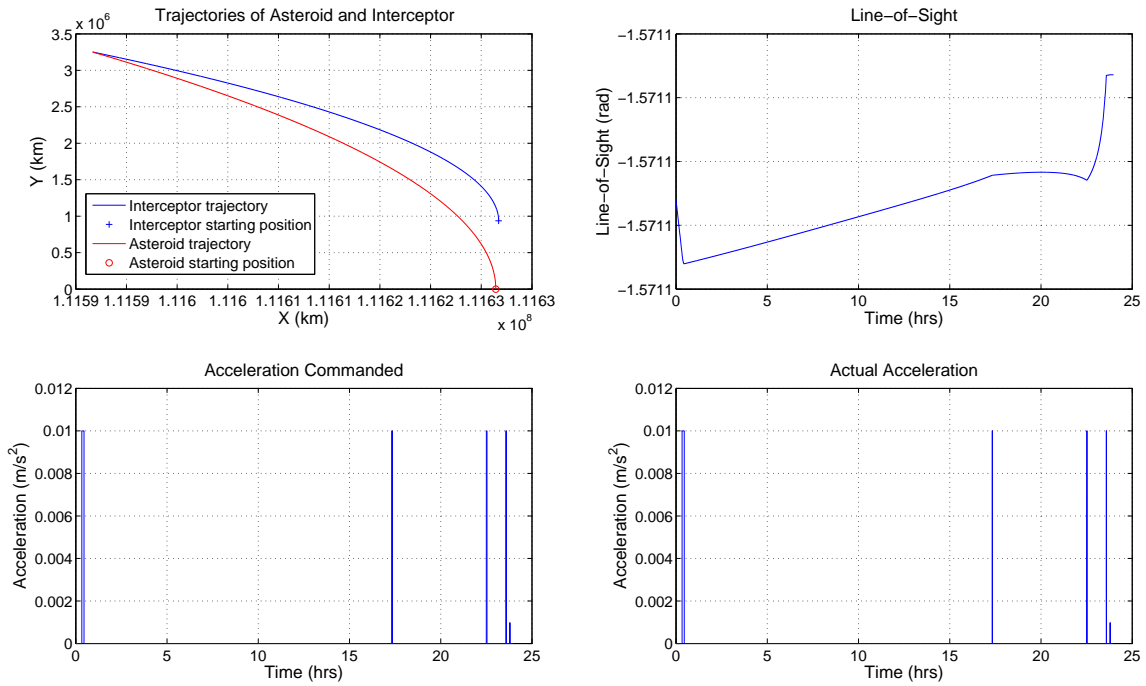


Figure 7. Trajectories, line-of-sight angle, commanded acceleration, and applied acceleration for OD guidance.

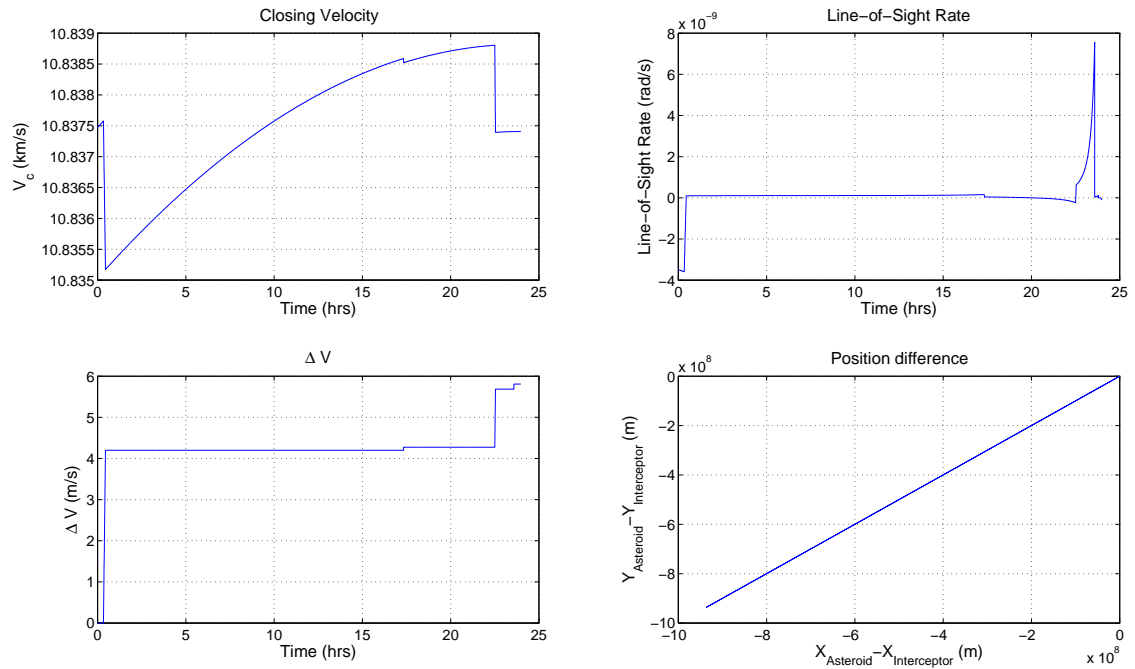


Figure 8. Closing velocity, line-of-sight rate, Δv used, and position difference for OD guidance.

Table 2. Initial Conditions.

body	x position, km	y position, km	x velocity, km/s	y velocity, km/s
Target	111.626×10^6	0	0	37.6301
Interceptor	111.627×10^6	936.358×10^3	0	26.7926

Table 3. Performance comparison of various guidance laws

Guidance Laws	Δv , m/s	ZEM, m
PN	5.67	4.27
Augmented PN	5.55	3.43
Pulsed PN	4.72	4.37
Pulsed Augmented PN	4.23	3.34
Predictive Impulsive	4.34	3.39
Kinematic Impulsive	4.34	4.87
Orbit Determination	5.81	6.11

Impact Angle Guidance

The impact angle guidance law was simulated for a variety of initial conditions and commanded angles. The results shown here are for a nominal 100 m/s relative impact velocity at a 0° approach angle. Approach angles were commanded from -90° to $+90^\circ$, in 15° increments. Table 4 gives the commanded approach angles, and the achieved approach angle and impact angle for each, as well as required Δv , achieved closing velocity (nominally 100 m/s), and total mission time from the nominal terminal mission start time (nominal case takes 24 hours).

Figure 9 shows the final impact velocity vectors for the range of angles. In this figure the asteroid’s heliocentric velocity is approximately straight up (positive y-axis), with the Sun to the left (negative x-axis).

For a guidance scheme which changes the approach angle significantly, the phase angle must be taken into account. For this analysis a simple model was used to simulate center-of-brightness motion due to the phase angle. The center of brightness corresponds to the center of the target for a 0° phase angle, moving across the object until it disappears off one side as the phase angle approaches -90° . A simple cosine dependence was used, meaning the distance from the edge to the center of brightness increased from zero for -180° phase, increasing to one target radius (i.e. at the center of mass) as the phase angle increased to 0° . This center of brightness was then mapped onto the point on the sphere intersected by the line-of-sight. The impact angle guidance law was again simulated for a variety of initial conditions and commanded angles, with simulated center-of-brightness motion. The results shown here are for the same nominal 100 m/s relative impact velocity at a 0° approach angle. Approach angles were commanded from -90° to $+90^\circ$, in 15° increments. Table 5 gives the commanded approach angles, and the achieved approach angle and impact angle for each, as well as required Δv , achieved closing velocity (nominally 100 m/s), and total

Table 4. Impact angle guidance performance.

$\lambda_{f,comm}$, deg	λ_f , deg	Impact angle, deg	Δv , m/s	V_c , m/s	Mission time, hrs
-90	-90.00	90.00	193.59	33.36	41.14
-75	-74.99	90.00	178.03	50.52	32.79
-60	-60.01	89.99	154.65	66.08	28.73
-45	-45.01	89.99	124.26	79.63	26.40
-30	-29.98	89.98	87.93	90.32	25.02
-15	-14.98	89.98	47.21	97.30	24.27
0	0.00	90.00	4.08	99.98	24.00
15	14.99	89.99	39.27	98.14	24.18
30	30.00	90.00	80.60	91.92	24.84
45	44.98	89.98	117.88	81.87	26.08
60	60.01	89.98	149.48	68.78	28.20
75	75.01	89.99	174.23	53.55	31.83
90	89.00	90.00	190.43	37.90	38.27

mission time from the nominal terminal mission start time (nominal case takes 24 hours).

Table 5. Impact angle guidance performance with center-of-brightness motion.

$\lambda_{f,comm}$, deg	λ_f , deg	Impact angle, deg	Δv , m/s	V_c , m/s	Mission time, hrs
-90	-90.06	88.18	193.61	33.29	41.14
-75	-74.90	82.63	178.04	50.45	32.79
-60	-59.80	74.46	154.75	65.99	28.73
-45	-44.81	66.57	124.36	79.54	26.40
-30	-29.81	58.78	88.03	90.23	25.02
-15	-14.84	51.07	47.35	97.21	24.27
0	0.13	43.36	4.29	99.91	24.00
15	15.12	35.60	39.49	98.07	24.18
30	30.14	27.69	80.80	91.87	24.84
45	45.14	19.47	118.08	81.84	26.08
60	60.13	10.52	149.66	68.77	28.20
75	75.03	1.61	174.36	53.54	31.83
90	88.80	7.93	190.56	37.90	38.26

Figure 10 shows the final impact velocity vectors for the range of angles. In this figure the asteroid's heliocentric velocity is approximately straight up (positive y-axis), with the Sun to the left (negative x-axis).

These results show a general trend among Δv requirements, closing velocity, and mission duration. Mission designers must consider the amount of extra fuel needed to allow larger and larger margins for approach angle change. Just as importantly, the closing velocity drops off significantly for the largest angle changes. The most extreme angle changes sacrifice much of their relative velocity by the time impact is achieved, and the payload being delivered

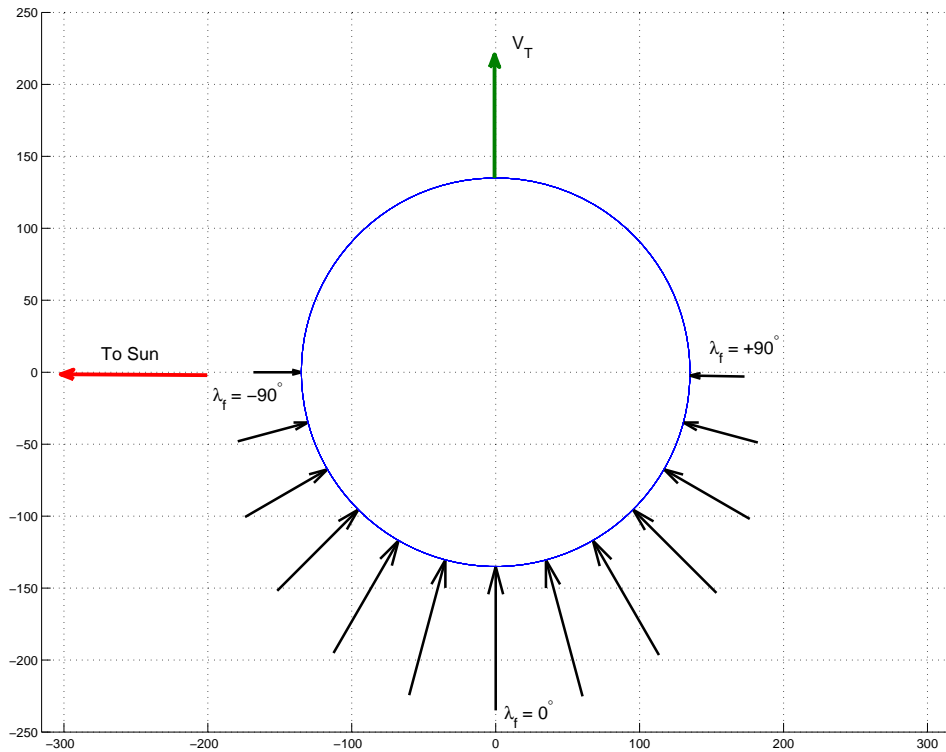


Figure 9. Terminal velocity vectors for a variety of commanded impact angles.

may have some minimum required relative velocity for effectiveness. The trend amongst the velocity vectors for the case with center-of-brightness motion is quite apparent and dramatic. Knowledge of the general trends when phase angle is relevant can help overcome observational deficiencies when much of the body is away from direct sunlight.

Leader/Follower Scheme

The leader-follower type configuration was simulated for a variety of initial conditions and guidance law types. The results shown here are for a nominal 10 km/s relative impact velocity at a 180° approach angle. Results are shown for proportional navigation guidance and for orbit determination guidance. The performance of the various impulsive guidance laws is similar, so orbit determination guidance is representative of all of the impulsive guidance laws.

For this first study of this type of sophisticated, high-velocity separation scheme, a number of assumptions and decisions must be made. It is not known what constitutes a “good” amount of separation time between the penetrator and the payload. Enough time must be allowed to avoid the disruptive initial shock waves that are troublesome for the nuclear payload, but not so much time that the hole bored through the asteroid closes in on itself. Based on some experience with hydrodynamic codes for simulating disruption events,¹⁴ it seems that times in the range of 1 to 5 seconds are appropriate. For a 10 km/s impact velocity, this represents a separation of 10 to 50 km. The results presented will be for the middle-ground 3-second case. Some assumptions are made on the release mechanism. It is

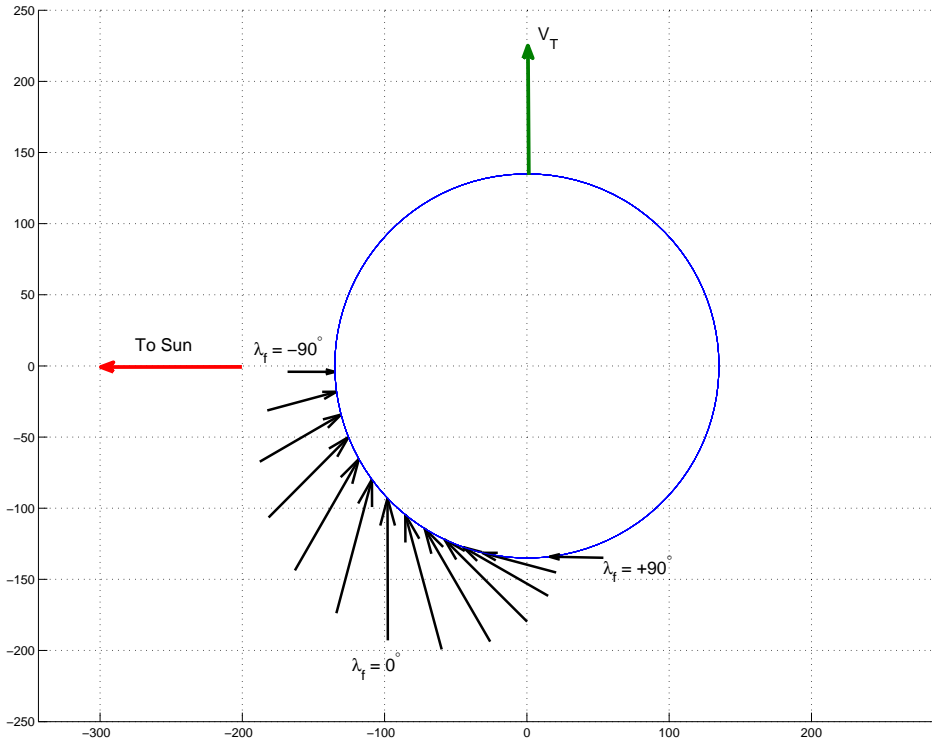


Figure 10. Terminal velocity vectors for a variety of commanded impact angles with center-of-brightness motion.

assumed that the release is clean. This represents the perfect case for release, or a slightly off-nominal case that the spacecraft’s attitude control systems can overcome. A 1-degree off-nominal separation is also simulated for the case of some release condition errors.

Two different release times are simulated. One is the “early” release, 24 hours before impact (thus at the beginning of the terminal mission phase). This represents a case where the two spacecraft should have enough time to compensate for the release conditions, with the risk of more time to introduce new errors in, for example, guidance command execution. The other time is the “late” release, only 30 minutes before impact. This represents a case where the spacecraft should already be on a collision course with no further accelerations needed, and the release event is needed merely to separate the craft an appropriate distance before impact time. Because the velocity change from such a separation event is large, the spacecraft will in fact need to command control accelerations to get back on a collision course. The early release option requires a separation velocity of 0.347 m/s to effect a 30 km (3 second) time delay at impact. The late release requires a 16.67 m/s separation velocity.

Two types of missions are simulated. In the “separate GNC” case, it is assumed that both spacecraft have a well-known center of brightness position available to them. The two craft are able to function independently to target the same center-of-brightness point on the asteroid. For the proportional navigation case, both spacecraft wait 100 seconds after separation to begin applying thrust. For the orbit determination case, the firing times are chosen so as not to conflict with separation.

The second mission type is the “beacon” case. In this case, the leader continues to apply normal guidance, while the follower follows a beacon on the leader. Its line of sight for guidance, then, is along the relative position vector between the two craft. As before, there is a 100 second delay after separation before applying proportional navigation. For orbit determination, there is a two-minute delay between the leader’s maneuver and the follower’s maneuver, to ensure that the follower is commanding to follow the leader’s new trajectory.

Parameters such as separation time, impulsive firing times, and proportional navigation guidance constant are not optimized for these cases. Rather, the cases are based on successful parameters for the simple intercept mission, and represent a range of reasonable parameters for a generic leader/follower intercept case with no a priori information about the particulars of the mission (separation time, delay, alignment errors, etc.).

It must be emphasized that for the early stages of this challenging new research area, many relevant factors are poorly known, if known at all. Issues like ideal separation time, observation quality for the follower, separation mechanism performance, and more are all the subject of current and future research. The values adopted for these cases should be seen as provisional. As research continues some of the values and assumptions may prove to be inaccurate, but this analysis should provide a good starting point for future work.

Table 6 gives the position difference between the leader and the follower for the various types of guidance described above. The radius of the target body is 135 meters. In cases where the offset distance is less than 135 meters, both craft hit the target. In the other cases, the leader impacted, but the follower did not. In all cases, when impact of both craft was achieved, the impact angles were within 0.5° of vertical, and the angle between the two craft was negligible for cases with small position offsets.

Table 6. Final position offset for various leader/follower missions.

Separation time	Guidance type	GNC computers	alignment error	Offset distance, m
early	OD	separate	no	0.122
early	OD	beacon	no	11700
early	OD	separate	yes	0.122
early	OD	beacon	yes	12000
early	PN	separate	no	0.005
early	PN	beacon	no	18.9
early	PN	separate	yes	0.005
early	PN	beacon	yes	18.5
late	OD	separate	no	797
late	OD	beacon	no	11.4
late	OD	separate	yes	1490
late	OD	beacon	yes	356
late	PN	separate	no	0.005
late	PN	beacon	no	4.32
late	PN	separate	yes	0.007
late	PN	beacon	yes	120

A wide range of offset distances result from the different mission design parameters. For orbit determination guidance, commanding to a nearby spacecraft results in large offsets for the early separation case. In late separation cases, the velocity change from separation proves to be a bit much to overcome for separate GNC, and commanding the follower to the leader's beacon works better. PN guidance performs quite well whenever the spacecraft have separate GNC systems. The beacon case tends to result in both craft hitting the target, but not near the same point. In practice the line-of-sight angular rate is quite small, so the acceleration levels are sensitive to small changes in the rate, and it is questionable if the GNC system will be able to actually realize such small measurements. With the beacon readily available and the small relative separation and velocity, some form of linearized velocity-to-gain guidance may be more appropriate.

CONCLUSION

The simulation results in this paper show the variety of guidance schemes available for different types of nuclear penetrator missions. An orbit determination scheme of the type used on NASA's successful Deep Impact mission is vital for formulating guidance laws to meet the wide variety of potential requirements for a nuclear penetrator mission. This orbit determination system provides significant amounts of information from only onboard optical measurements.

Angle-of-impact guidance can be used for low relative velocity missions when the ability to drastically change the mission approach angle at the last minute is desirable. A range of different approach angles are achievable with an amount of fuel that an interceptor spacecraft could carry on-board. Adverse lighting may occur when significantly changing the phase angle towards the end of operations. Although the lighting situation presented will be different for each asteroid, knowledge of the general way in which the center of brightness moves due to a changing phase angle can be used to alleviate some of the deleterious effects of such center of brightness motion. Mission designers are not restricted to a narrow envelope of approach angles if fuel can be carried to change this approach angle at a later time.

Preliminary studies of a new type of mission for high-speed autonomous spacecraft operating in tandem show that this method has promise as a way of effectively delivering a subsurface nuclear device to an asteroid, thus maximizing the energy coupling from the device to the asteroid. The general feasibility of this method has been shown for both impulsive and low-thrust guidance laws. A number of potential roadblocks need to be researched, ranging from spacecraft sizing to attitude control to the physics of high speed penetrator devices. A framework to start studying this new topic is established.

ACKNOWLEDGMENT

This research work was supported by a research grant from the Iowa Space Grant Consortium (ISGC) awarded to the Asteroid Deflection Research Center at Iowa State University. The authors would like to thank Dr. Ramanathan Sugumaran (Director of the ISGC) for his support of this research work.

REFERENCES

- [1] *Defending Planet Earth: Near-Earth Object Surveys and Hazard Mitigation Strategies, Final Report, Committee to Review Near-Earth Object Surveys and Hazard Mitigation Strategies, National Research Council.* The National Academies Press, January, 2010.
- [2] J. P. Sanchez, M. Vasile, and G. Radice, “On the Consequences of a Fragmentation Due to a NEO Mitigation Strategy,” Glasgow, UK, IAC-09-C1.3.1, 59th International Astronautical Congress, 2008.
- [3] B. D. Kaplinger, B. Wie, and J. P. Basart, “A Preliminary Study on Nuclear Standoff Explosions for Deflecting Near-Earth Objects,” Granada, Spain, 1st IAA Planetary Defense Conference, 2009.
- [4] B. D. Kaplinger, B. Wie, and D. Dearborn, “Preliminary Results for High-Fidelity Modeling and Simulation of Orbital Dispersion of Asteroids Disrupted by Nuclear Explosives,” Toronto, Canada, AIAA 2010-7982, AIAA/AAS Astrodynamics Specialist Conference, 2010.
- [5] R. B. Frauenholz, R. S. Bhat, S. R. Chesley, N. Mastrodemos, W. M. O. Jr., and M. S. Ryne, “Deep Impact Navigation System Performance,” *Journal of Spacecraft and Rockets*, Vol. 45, No. 1, 2008, pp. 39–56.
- [6] B. Wie, “Astrodynamics Fundamentals for Deflecting Hazardous Near-Earth Objects,” *John Breakwell Memorial Lecture*, Daejeon, Korea, IAC-09-C1.3.1, 60th International Astronautical Congress, 2009.
- [7] M. Hawkins, A. Pitz, B. Wie, and J. Gil-Fernández, “Terminal-Phase Guidance and Control Analysis of Asteroid Interceptors,” Toronto, Canada, AIAA 2010-7982, AIAA/AAS Astrodynamics Specialist Conference, 2010.
- [8] D. G. Kubitschek, N. Mastrodemos, R. A. Warner, S. P. Synnott, S. Bhaskaran, J. E. Riedel, B. M. Kennedy, G. W. Null, and A. T. Vaughan, “The Challenges of Deep Impact Autonomous Navigation,” *Journal of Field Robotics*, Vol. 24, No. 4, 2007, pp. 339–354.
- [9] J. E. Riedel, S. Bhaskaran, D. B. Eldred, R. A. Gaskell, C. A. Grasso, B. Kennedy, D. Kubitschek, N. Mastrodemos, S. P. Synnott, A. Vaughan, and R. A. Werner, “AutoNav Mark3: Engineering the Next Generation of Autonomous Onboard Navigation and Guidance,” Jet Propulsion Laboratory, Pasadena, CA, USA, 2006.
- [10] M. Kim and K. V. Grider, “Terminal Guidance for Impact Attitude Angle Constrained Flight Trajectories,” *IEEE Transactions on Aerospace and Electronic Systems*, Vol. 9, No. 6, 1973, pp. 583–859.
- [11] P. Zarchan, *Tactical and Strategic Missile Guidance*, Vol. 219 of *Progress in Astronautics and Aeronautics*. AIAA, Reston, VA, fifth ed., 2007.
- [12] V. G. Chistov, P. V. Grigal, A. G. Lyubimov, B. V. Zamyshlyaev, and A. A. Taranov, “Nuclear Explosive Deep Penetration Method into Asteroid,” Proceedings of the Chelyabinsk Scientific Center. Special Issue: Space Protection of the Earth., 1997.
- [13] D. S. Dearborn, “21st Century Steam for Asteroid Mitigation,” Orange County, CA, USA, 2004 Planetary Defense Conference: Protecting Earth from Asteroids, 2004.
- [14] B. Wie and D. Dearborn, “Earth-Impact Modeling and Analysis of a Near-Earth Object Fragmented and Dispersed by Nuclear Subsurface Explosions,” *AAS 10-137*, San Diego, CA, 20th AAS/AIAA Space Flight Mechanics Meeting, 2010.